Characterization of the Hydrolysis Mechanism of Polyalternating Alginate in Weak Acid and Assignment of the Resulting MG-Oligosaccharides by NMR Spectroscopy and ESI−Mass Spectrometry

Synnøve Holtan,* Qiujin Zhang, Wenche Iren Strand, and Gudmund Skjåk-Bræk

Norwegian Biopolymer Laboratory, Department of Biotechnology, The Norwegian University of Science and Technology (NTNU),Sem Sælands vei 6/8, N-7491 Trondheim, Norway

Received December 22, 2005; Revised Manuscript Received April 24, 2006

Alginate with long strictly alternating sequences of mannuronic (M) and guluronic (G) acid residues, $F_G = 0.47$ and $F_{GG} = 0.0$, was prepared by incubating mannuronan with the recombinant C-5 epimerase AlgE4. By partial acid hydrolysis of this PolyMG alginate at pH values from 2.8 to 4.5 at 95 °C, α-L-Gul*p*A-(1→4)-*β*-D-Man*p*A (G−M) linkages were hydrolyzed far faster than *β*-D-Man*p*A-(1→4)-α-L-Gul*p*A (M−G) linkages in the polymer chain. The ratio of the rates (k_{G-M}/k_{M-G}) decreased with increasing pH. The dominant mechanism for hydrolysis of (1→4)-linked PolyMG in weak acid was thus proved to be an intramolecular catalysis of glycosidic cleavage of the linkages at C-4 by the undissociated carboxyl groups at C-5 in the respective units. The higher degradation rate of G−M than M−G glycosidic linkages in the polymer chain of MG-alginate at pH 3.5 and 95 °C was exploited to make oligomers mainly consisting of M on the nonreducing and G on the reducing end and, thus, a majority of oligomers with an even number of residues. The ratio of the rate constants k_{G-M}/k_{M-G} at this pH was 10.7. The MG-hydrolysate was separated by size exclusion chromatography and the MG oligosaccharide fractions analyzed by electrospray ionization−mass spectrometry together with ^{1}H and ^{13}C NMR spectroscopy. Chemical shifts of MG-oligomers (DP2−DP5) were elucidated by 2D ^{1}H and ^{13}C NMR.

Introduction

Alginate is a collective term for a family of polysaccharides produced by brown algae[1] and some bacteria.[2,3] Chemically, they are linear copolymers of (1→4)-linked *β*-D-mannuronic acid (M) and its C-5 epimer α-L-guluronic acid (G), arranged in a blockwise pattern along the chain with homopolymeric (MM or GG) or heteropolymeric (MG) regions. The composition and sequential arrangements vary widely from homopolymeric mannuronan to polymers with >70% guluronic acid. Apart from mannuronan, most naturally occurring alginates do not exhibit a repeating unit nor can their sequence be described by Bernoullian statistics. In its biosynthetic pathway, the binary block structure in alginate is produced in a post- polymerization reaction involving a C-5 inversion on the M residues of mannuronan into guluronic acid. This reaction is catalyzed by the mannuronan C-5 epimerases. The alginate producing bacterium *Azotobacter vinelandii* encodes seven secreted Ca^{2+} dependent epimerases designated AlgE1−AlgE7, which have been sequenced, cloned, and produced recombinantly in *Escherichia coli*.[4,5,6] Each of these recombinant enzymes generates specific nonrandom epimerization patterns when acting upon mannuronan or alginate as substrate. The AlgE4 epimerase forms alginates with long strictly alternating sequences as shown in Figure 1, whereas the action of AlgE1 and AlgE6 generates long G-blocks.[6−10] The availability of these alginate- modifying enzymes makes it possible to tailor alginates with virtually regular structures, such as PolyM, PolyMG, and PolyG.[11]

Acid hydrolysis has been widely used as a tool for studying the chemical composition and structure of polysaccharides. The difference in rates of hydrolysis of the various glycosidic linkages in the polysaccharide allows the isolation and characterization of oligosaccharide fractions. The mechanism of hydrolysis of glycosides is generally thought to involve three steps: (1) A protonation of the glycosidic oxygen to give the conjugate acid; this step is rapid and the acid will exist in its equilibrium concentration. (2) A unimolecular heterolysis of the conjugate acid with the formation of a nonreducing end group and a carbonium-oxonium ion; this step is slow and rate determining. (3) A rapid addition of water to the carbonium-oxonium ion with the formation of a reducing end group and a proton. At low pH values the linkages between uronic acid residues are more stable than those for neutral sugars.[14] This is due to an inductive effect of the carboxyl group, lowering the concentration of conjugate acid (step 1) and decreasing the rate of electron transfer in step 2. In pectins, the preferential cleavage of the linkages between galacturonic acid and rhamnose (neutral sugar) at pH values <2 has been used to study the length of the homogalacturonic regions of the backbone.[12] In the case of alginate, the isolation of three fractions with different chemical composition, an M- (approximately 90% M), a G- (approximately 90% G), and an MG-fraction (approximately 55−60% M), by partial acid hydrolysis of algal alginate, demonstrated the blockwise arrangement of uronic acids along the chains of the polymer.[13] The mechanism of hydrolysis of M-, G-, and MG-enriched alginate fragments has further been studied at pH values above 2, where the degradation rates depend only slightly upon hydrogen ion activity and are much higher than for neutral polysaccharides under the same conditions.[14−16] Degradation rate constants were determined by measuring the increase in reducing power of the solutions as a function of time. Oligomannuronic acids ($DP_n \approx 5$) were hydrolyzed faster than oligoguluronic acids ($DP_n \approx 3.5$) and the respective rate

* Corresponding author. Tel.: + 47 69 11 86 39. Fax: + 47 69 11 88 45. E-mail: synnove.holtan@borregaard.com.

10.1021/bm050984q CCC: $33.50
Published on Web 06/09/2006

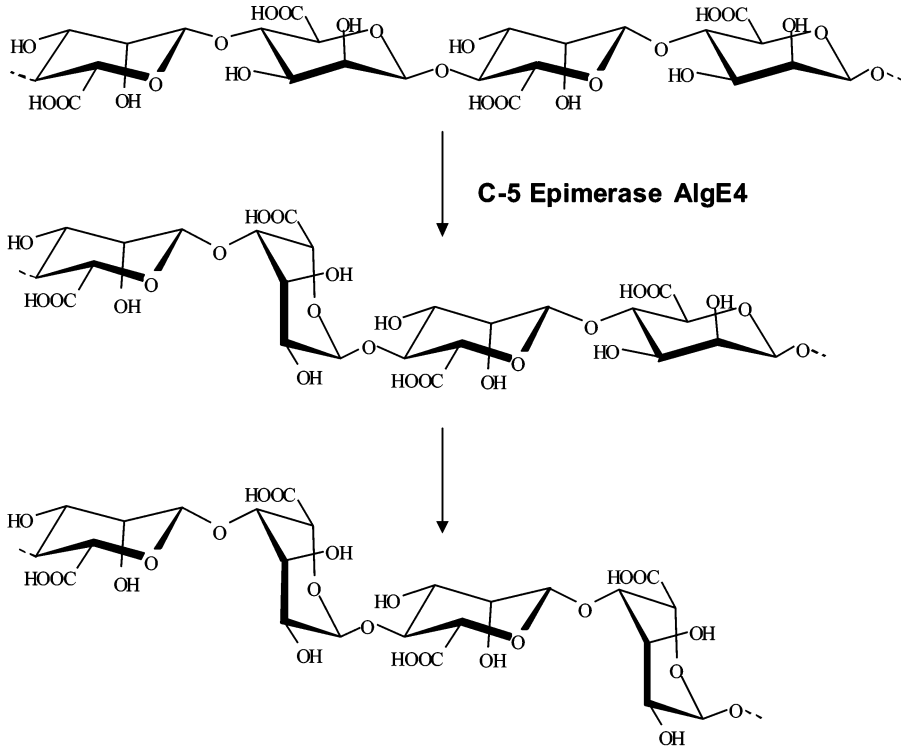

→4)-β-D-Man*p*A-(1→4)-α-L-Gul*p*A-(1→4)-β-D-Man*p*A-(1→4)-α-L-Gul*p*A-(1→

Figure 1. Epimerization of a mannuronan segment with the mannuronan C-5 epimerase AlgE4.

constants k_M and k_G followed a first-order reaction, the ratio k_M/k_G having a maximum of about 4.3 at pH 2.8 and 100 °C. Oligouronides containing both monomers M and G ($DP_n \approx 20$) were hydrolyzed at intermediate rates, giving curved lines when the results were plotted according to a first order reaction. For the predominantly alternating material it was found that the mannuronic acid residues were exposed as nonreducing terminal groups considerably faster than the guluronic acid residues. The marked divergence in the rates of hydrolysis of oligomannuronic and oligoguluronic acids was therefore attributed mainly to an influence of the configuration at C-5 of an uronic acid residue upon the rate of cleavage of the glycosidic linkage attached to C-4 of the same residue. The high rate of hydrolysis of (1→ 4) linked polyuronides in weakly acidic media was further shown to be due to an intramolecular catalysis of glycosidic cleavage either by the dissociated carboxyl groups assisting proton catalyzed hydrolysis or most probably by the undissociated carboxyl groups acting directly as proton donors.

The novel tuning of alginate composition and sequential structure, combined with the quantitative detection of reducing end resonances by high field NMR spectroscopy during the hydrolysis reaction, enables us to calculate the rate constants for degradation of the various glycosidic linkages individually. In the present paper, strictly alternating alginate (PolyMG) with $F_G = 0.47$ and $F_{GG} = 0.0$ is obtained by treating mannuronan with the C-5 epimerase AlgE4. This enzyme has shown to have a processive mode of action epimerising on average 10 residues for each enzyme- substrate encounter.[17] The difference in rates of hydrolysis of M−G and G−M glycosidic linkages in alginates in weak acid at 95 °C is examined according to the monomers respective pK_a values and the conformation of the disaccharide subunits constituting the susceptible linkages; →4)-*β*-D-Man*p*A-(1→4)-α-L-Gul*p*A-(1→ and →4)-α-L-Gul*p*A-(1→4)-*β*-D-Man*p*A-(1→, by degrading PolyMG at various pH values and analyzing the composition of the hydrolysates as a function of time by ^{1}H NMR spectroscopy.

For utilization in structural work examining the mode of action and the subsite size and specificity of G-block forming mannuronan C-5 epimerases and of different alginate degrading enzymes (lyases), the demand for uniform MG-oligomers of various degrees of polymerization for use as substrates is raised.[11,17] The faster degradation of G−M linkages than M−G linkages is here exploited to make MG-oligomers that mainly consist of M on the nonreducing and G on the reducing end by hydrolysis of PolyMG alginate at pH 3.5 and 95 °C. The MG-hydrolysate is separated by size exclusion chromatography (SEC), followed by characterization of the oligosaccharide fractions by high resolution 2D NMR spectroscopy and electrospray ionization−mass spectrometry (ESI-MS).

Experimental Section

Alginate. High molecular mass mannuronan was isolated from the fermentation broth of an epimerase-negative strain[18] of *Pseudomonas fluorescens*. Purification and deacetylation were carried out as described previously.[19] No guluronate signals could be detected by ^{1}H NMR (molar fraction of guluronic acid $F_G < 0.001$), indicating a homopolymeric mannuronan.

A ^{13}C-labeled mannuronan was produced by growing the mannuronan producing *P. fluorescens* strain on agar plates with D-[1-^{13}C]fructose (99%) as the carbon source. The medium contained peptone (Oxoid L37) 20 g/L, $MgCl_2 \cdot 6H_2O$ 1.4 g/L, NaCl 5 g/L, D-[1-^{13}C]-fructose (Cambridge Isotope Lab., Massachusetts, U.S.A.), 3 g/L. The plates were incubated for 48 h at 20 °C and then for another 72 h at 6 °C. The polymer was harvested and purified. The mannuronan product was selectively enriched to 59% ^{13}C in the C-1 position.[9]

Enzyme. The mannuronan C-5-epimerase AlgE4 with a molecular mass of 57.7 kDa was produced by fermentation of a recombinant *E. coli* strain JM 105.[7] The enzyme was partly purified by ion-exchange chromatography on Q-Sepharose FF (Pharmacia, Uppsala, Sweden) and by hydrophobic-interaction chromatography on Phenyl Sepharose FF (Pharmacia). The activity of the enzyme was assayed by measuring the release of tritium to water, when ^{3}H-5-labeled mannuronan was incubated with the enzyme.[19]

C-5 Epimerization. Mannuronan was dissolved in deionized (MQ) water overnight before a concentrated stock solution of MOPS (3-[N-morpholino]-propanesulfonic acid) buffer, pH 6.9 with $CaCl_2 \cdot 2H_2O$ and NaCl was added and the mixtures preheated at 37 °C. The AlgE4 enzyme was dissolved in MQ−water and immediately added to the alginate solution. Final concentrations of the reaction mixtures were 0.25% (w/v) alginate, 50 mM MOPS buffer, 2.5 mM Ca^{2+}, and 10 mM NaCl. The molar ratio of enzyme: uronic acid residue was 1:60000. The mixtures were kept at 37 °C for 24 h, before the reaction was terminated on ice by addition of HCl until the pH was below 3. Following epimerization, the resulting alginates were purified by dialysis against 0.05 M HCl and finally against MQ- water until the conductance was below 4 μS at 4 °C.

Acid Hydrolysis (Kinetic Experiments). 0.25% (w/v) solutions of PolyMG-alginate and mannuronan in MQ−water were prehydrolyzed for 3.5 and 6 h respectively at pH 5.6 and 95 °C (step 1 of hydrolysis procedure), to visualize reducing end resonances by NMR from the start of the kinetic hydrolysis experiments. N_2-bubbling of the alginate solutions was used to remove O_2 prior to incubation at 95 °C. After neutralization and freeze-drying, solutions of the two alginates (2.0% w/v in MQ−water) were prepared and acidified with HCl to pH 2.8, 3.5, 4.0, and 4.5 for PolyMG and pH 3.5 for mannuronan. These pH-adjusted stock solutions were divided into a series of samples hydrolyzed for selected time periods at 95 °C. The hydrolysis reactions were stopped on ice and the samples were freeze-dried, pH adjusted (p^2H 5.5), and analyzed by ^1H NMR spectroscopy.

Acid Hydrolysis (Large Batch). Partial acid hydrolysis of a large batch of PolyMG-alginate 0.25% (w/v) solution in MQ−water was performed in two steps. First, the pH of the solution was adjusted to 5.6 with 0.1 M HCl, prior to deoxygenation with nitrogen, followed by incubation at 95 °C for 3.5 h to undergo prehydrolysis. The sample was then cooled, pH adjusted to 3.5 with 0.1 M HCl, degassed, and hydrolyzed at 95 °C for 4 h (step 2). After this period, the sample was immediately cooled on ice, neutralized (pH 7) by addition of 0.1 M NaOH, and freeze-dried.

Size Exclusion Chromatography. The PolyMG-hydrolysate was fractionated according to its chain-length on three columns of Superdex 30 preparative grade (HiLoad 2.6 × 60 cm, serially connected, Pharmacia) at a flow rate of 0.8 mL/min with 0.1 M NH_4Ac (pH 6.9) at room temperature. An on-line refractive index (RI) detector (Shimadzu RID-6A) was used to measure the relative concentration of oligomers eluting from the column. Fractions of 5 mL were collected from three successive column runs and pooled on the basis of peaks identified from the RI profile. These pooled samples were stored at 4 °C prior to three cycles of freeze-drying to remove all traces of NH_4-Ac and to provide solid, purified MG-oligomers (F2−F16).

NMR Spectroscopy. ^1H NMR spectra were recorded on a Bruker Avance DPX 300 or 400 spectrometer at 90 °C. Spectra were obtained using a pulse repetition time of 5.6 s and a 30° pulse angle. Sample concentrations of 10 mg/mL (1.0% w/v) in deuterium oxide (^2H_2O) were used, and the chemical shift was calculated with respect to 3-(trimethylsilyl)-propionic-2,2,3,3-d_4 acid sodium salt (TSP, Aldrich, Milwaukee, WI) as the internal standard. Peaks of high molecular mass samples were assigned according to Grasdalen.[20]

^{13}C NMR spectra were recorded on a Bruker Avance DPX 400 spectrometer operating at 100 MHz and 90 °C. A pulse repetition time of 2.2 s and a 30° pulse angle were used. To reduce the viscosity of the high molecular mass C-1 ^{13}C-labeled PolyMG for high-resolution NMR analysis, the sample was degraded by mild acid hydrolysis[19] to a final DP_n of approximately 30. An aqueous solution of 0.5 mg/mL alginate (0.05% (w/v)) at pH 5.6 was kept for 60 min in a water bath at 95 °C, and then the pH was adjusted to 3.8 and the solution kept for 40 min at 95 °C.

^1H NMR Monitored Hydrolysis Reaction. The PolyMG-alginate (0.25% (w/v) solution in MQ−water) was prehydrolyzed for 1 h at pH 5.6 and 95 °C to reduce the viscosity of the sample prior to the time resolved ^1H NMR experiment. Following freeze-drying, a solution of this pre- treated PolyMG in ^2H_2O (2.0% w/v) was adjusted to a p^2H of 4.0 with deuterium chloride (^2HCl). To monitor the progress of degradation of the sample, a series of 60 successive ^1H NMR spectra were recorded at 95 °C. The procedure was automated by using the multizg command. Spectra were obtained using a 30° pulse angle, a spectral width of 3000 Hz, and a data-block size of 32 K; 128 scans were accumulated after 4 dummy scans. The resulting time interval between two successive spectra was 14.4 min.

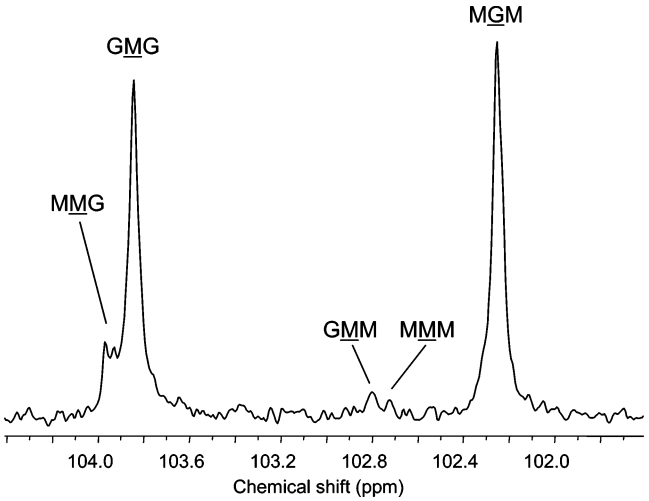

Figure 2. ^{13}C NMR (100 MHz) spectrum of C-1 ^{13}C-labeled PolyMG ($F_G = 0.47$, $F_{GG} = 0.0$).

1D and 2D NMR Experiments for Structure Analysis. To make a complete assignment of the ^1H and ^{13}C peaks of purified alginate samples with low degree of polymerization, high resolution ^1H- and ^{13}C-1D NMR, homonuclear 2D NMR ($^1H-^1H$ COSY and $^1H-^1H$ TOCSY) and heteronuclear 2D NMR ($^1H-^{13}C$ HSQC and $^1H-^{13}C$ HMBC) spectra were performed on a Bruker Avance 600 spectrometer equipped with CryoProbe. The resonance frequency is 600.13 MHz for ^1H and 150.92 MHz for ^{13}C, respectively. All samples were recorded at room temperature except for the pentamer, which was recorded at 295 K in order to avoid overlap between the ^1H signal in ^2H_2O and sample peaks. ^1H NMR spectra of oligomers were obtained by presaturating the residual proton signal from solvent with a weak pulse. The pulse sequence with double quantum filter and phase sensitivity was used for COSY experiment. Gradient-selected pulse sequences were used for TOCSY, HSQC, and HMBC experiments. Experimental parameters, such as $\pi/2$ pulse-width, spectral width, data points in time domain, and scan number, were optimized for each observed sample individually. The duration of spin-lock was set to 100 ms for TOCSY experiments. A compromised one-bond $^{13}C-^1H$ spin coupling constant of 155 Hz was set for HSQC and HMBC experiments.

ESI-MS. Samples were dissolved in MQ−water and diluted in 50% aqueous methanol containing formic acid (0.5%) in positive mode and 50% aqueous methanol containing ammonia (1%) in negative mode. Sample concentrations of 0.01−0.02% (w/v) were analyzed by direct infusion (0.6 mL/h) into an Agilent MSD Trap SL mass spectrometer equipped with an electrospray ion source. The drying gas flow was 4 L/min, the drying gas temperature was 325 °C, and the nebulizer pressure was 15 lb/in.^{2}. The capillary voltage was 3.5 kV in negative-ion mode with an endplate offset of −0.5 kV. In positive-ion mode, capillary voltages of −3.5 or −4 kV were used.

Results and Discussion

PolyMG-Alginate. A ^{13}C NMR spectrum (100 MHz) of the anomeric region of C-1 ^{13}C-labeled mannuronan fully epimerised with AlgE4 is shown in Figure 2. The signals from the anomeric carbons appear in the range of 102−104 ppm, where both the neighboring residues in the alginate chain influence

the chemical shifts significantly. Peaks are assigned according to refs 17, 21, and 22 and indicated in Figure 2, where MMM represents triads in unepimerised regions, GMG and MGM indicate triads within blocks of alternating sequences, and MMG and GMM represent triads at the beginning and the end of an MG block. The observed residue is marked with an underline. The integrated intensity of these signals allows us to calculate the molar fraction of the triads; F_{MMM}, F_{GMG}, F_{MGM}, F_{MMG}, and F_{GMM}. From the dominant resonance signals from the triads GMG and MGM in the spectrum, it is clear that the labeled mannuronan homopolymer has been converted to a heteropolymer of mannuronic and guluronic acid residues composed in a strictly alternating manner by in vitro epimerization with AlgE4. The small peaks from the asymmetric triads, MMG and GMM, prove the presence of long alternating MG blocks. Quantitatively, the molar fraction of G residues (F_G) is calculated to be 0.47. No signals from two consecutive G residues were observed within the sensitivity of the NMR experiment ($F_{GG} = 0.0$). The average M block length ($N_{M>1}$) stemming from the residual unepimerised M residues and 6% higher M than G content in the PolyMG-alginate was calculated to approximately 2, by the equation $N_{M>1} = F_M - F_{GMG}/F_{MMG}$.[22]

In our previous study,[17] the average number of repeating units in the [MG] blocks was calculated and found to be larger than 20 for a fully epimerised PolyMG-alginate with $F_G = 0.47$. Recently, a statistical simulation of the block length and distribution of the extra 6% MM content in the PolyMG ($F_G = 0.47$ and $F_{GG} = 0.0$) has been carried out based on the weight distribution of chain lengths in a PolyMG-hydrolysate obtained by HPAEC−PAD.[23] Taking the difference in rates of degradation of the glycosidic linkages into account, PolyMG was here estimated to have an average MG block length of around 38 monomer units and a polydisperse distribution of M blocks with an average length of 3.4, where the fraction of dimer (MM) is the most abundant constituting 41% of total M blocks. In the present paper, taking the prehydrolysis of PolyMG prior to ^{13}C NMR spectroscopy into account, the calculated average M block length could easily be underestimated due to hydrolyzed M−M linkages. Moreover, an average of approximately two consecutive M residues is in agreement with the most abundant chain-length of M residues in PolyMG, as reported by Ballance et al.[23]

NMR Monitored Acid Hydrolysis of PolyMG-Alginate. The progress of degradation of PolyMG was monitored by online ^1H NMR spectroscopy at p^2H 4.0 and 95 °C for 16 h. The ^2HCl adjusted p^2H value of 4.0 (corresponding to pH 4.4 according to Glasoe and Long)[24] was selected in order to avoid overlap between G-1 (i.e., H-1 of G residues) reducing end β and G-5M internal resonance signals in the ^1H NMR spectra occurring at lower p^2H values. The polymer was pre-hydrolyzed to a DP_n between 50 and 100 to visualize the reducing end signals from the start of the monitored hydrolysis experiment. From the time resolved ^1H NMR spectra (400 MHz) shown in Figure 3, a significant increase in signal intensities for G reducing end resonances; G-$1_{red}\alpha$ at 5.21 ppm, G-$1_{red}\beta$ at 4.86 ppm, G-$5_{red}\alpha$ at 4.64 ppm, and G-$5_{red}\beta$ at 4.42 ppm, and a similar decline in internal G-1, G-5M, and M-1G signal intensities is observed as a function of hydrolysis time. The splits in internal G-5M and M-1G signals and increasing peaks at 4.78 and 4.70 ppm, respectively, constitute the resonance signals from the nonreducing ends and residues preceding reducing ends. The M reducing end resonance signals, M-$1_{red}\alpha$ at 5.24 ppm and M-$1_{red}\beta$ at 4.89 ppm, increase only slightly during the degradation experiment. These results demonstrate

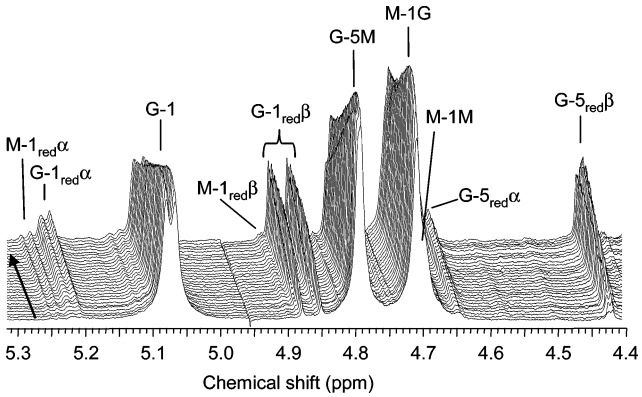

Figure 3. Stacked plot of ^1H NMR (400 MHz) spectra recorded during acid hydrolysis of PolyMG in ^2H_2O at p^2H 4.0 and 95 °C. The reaction was carried out inside the spectrometer. M-$1_{red}\alpha$, M-$1_{red}\beta$, G-$1_{red}\alpha$, and G-$1_{red}\beta$ denote H-1 in reducing end ManA and GulA residues, respectively. G-$5_{red}\alpha$ and G-$5_{red}\beta$ denote H-5 in reducing end GulA residues. The spectra shown were recorded in 29-min intervals, and within 14.5 h the DP_n decreased from approximately 40 in the first spectrum (1.5 h reaction time) to 4.2 in the last.

that the →4)-α-L-Gul*p*A-(1→4)-β-D-Man*p*A-(1→ glycosidic linkages in the PolyMG chain are hydrolyzed at a far higher rate than the →4)-β-D-Man*p*A-(1→4)-α-L-Gul*p*A-(1→ linkages, in agreement with Smidsrød et al.[16] No signals for unsaturated 4-deoxy-L-*erythro*-hex-4-enepyanosyluronate residues at the nonreducing end were detected within the sensitivity of the NMR experiment, indicating no noteworthy degradation by β-elimination mechanism. This has previously been reported for thermal degradation of solid-state alginate at pH 4.3;[25] however, the poor pH control for solid-state alginate could explain this.

The large number of spectra recorded during the hydrolysis of PolyMG allowed for a detailed analysis of the reaction kinetics and made it possible to reduce statistical errors occurring in the measurement and integration of signals. To determine the rate of degradation of the two linkages G−M and M−G in the polymer individually, the degrees of scission α_G and α_M, representing the fractions of G and M reducing ends of total guluronic and mannuronic acid residues respectively, were calculated from the ^1H NMR resonances as a function of time. To calculate the molar fraction of G at the reducing end (F_{Gred}), the intensities of the G-$1_{red}\beta$ and G-$5_{red}\alpha$ signals were used, due to the overlap of the G-$1_{red}\alpha$ peaks at 5.21 ppm with several undefined doublet peaks arising in this area with increasing degradation time (discussed further in following sections). The molar fraction of M at the reducing end (F_{Mred}) was calculated by using the intensities of the M-$1_{red}\alpha$ and M-$1_{red}\beta$ signals. Assuming the time dependent degradation of the two polymer linkages G−M and M−G considered separately will follow first-order kinetics, the rate constants k_{G-M} and k_{M-G} designating the rates of exposure of residues G and M, respectively, as reducing end groups, can be found by plotting $-\ln(1 - \alpha)$ for calculated values of α_G and α_M, as a function of time at p^2H 4.0 and 95 °C, see Figure 4. For hydrolysis of both G−M and M−G linkages by time up to 16 h and an average DP_n of hydrolysate of 4.2 examined, straight lines were obtained. The rate constants k_{G-M} and k_{M-G} determined from the slope of curves are given in Table 1. From Figure 4, it can be seen that linear regression of the curve for k_{M-G} gave a $R^2 = 95\%$. The lower accuracy in integrations of much lower signal intensities for M reducing ends, compared to those for G reducing ends ($R^2 \approx 100\%$), could explain this poorer regression fit. The ratio of the degradation rates (k_{G-M}/k_{M-G}) was 15.6 in this experiment.

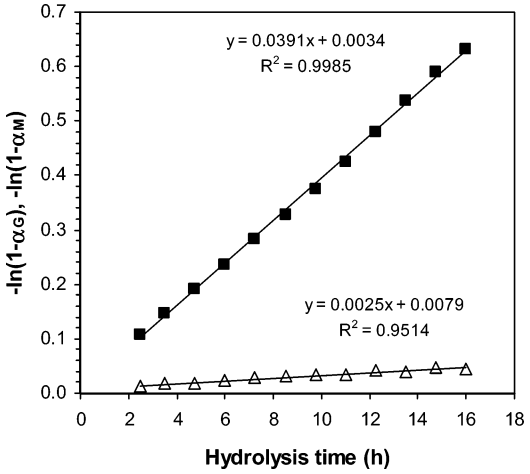

Figure 4. Rate of degradation of G−M (■) and M−G (△) glycosidic linkages in PolyMG at p^{2}H 4.0 and 95 °C. The respective rate constants, k_{G-M} (■) and k_{M-G} (△), were determined from the slope of the curves.

Table 1. Respective Rate Constants for Degradation of G−M (k_{G-M}) and M−G (k_{M-G}) Glycosidic Linkages in PolyMG According to the pH of the Solution[a]

PolyMG				
pH	k_{G-M}	k_{M-G}	k_{G-M}/k_{M-G}	k_{PolyMG} ($k_{G-M}F_G + k_{M-G}F_M$)
2.8	0.0755	0.0059	12.8	0.039
3.5	0.0483	0.0045	10.7	0.025
4.0	0.0279	0.0032	8.7	0.015
4.5	0.0128	0.0019	6.7	0.007
p^{2}H 4.0	0.0391	0.0025	15.6	0.020
3.5[b]	0.0319	0.0031	10.3	0.017

Mannuronan	
pH	k_{M-M}
3.5	0.0128

[a] PolyMG ($F_G = 0.47$, $F_{GG} = 0.0$) was hydrolyzed in weak acids, and for each pH, the hydrolysate composition by time was analyzed by ^{1}H NMR (300 MHz) spectroscopy. The signal intensities of G and M reducing end resonances were used to calculate the degrees of scission, α_G and α_M, respectively, and the rate constants k_{G-M} and k_{M-G} were found from the slope of the curve for $-\ln(1-\alpha)$ against time. The rate constants achieved by performing the hydrolysis of PolyMG at p^{2}H 4.0 in the NMR spectrometer, at an increased ionic strength of the solution at pH 3.5 and for mannuronan ($F_M = 1.0$) at pH 3.5 (k_{M-M}), are also shown. [b] 0.15 M NaCl.

Hydrolysis of PolyMG at Different Acidities. Following confirmation of respective first-order rate constants for G−M and M−G cleavage in weak acid of p^{2}H 4.0, kinetic experiments of the hydrolysis reaction of PolyMG in H_2O/HCl at 95 °C were performed. The degradation at four different acidities pH 2.8, 3.5, 4.0, and 4.5, below and above the pK_a values of 3.38 and 3.65 for M and G monomers, respectively,[26] were examined. The respective hydrolysates from selected time points were adjusted to p^{2}H 5.5 and analyzed by ^{1}H NMR spectroscopy. The progress of degradation of PolyMG at pH 3.5 is shown in Figure 5 by the^{1}H NMR spectra recorded from 1.5 to 15 h reaction time at 95 °C. For visualization and better calculation of reducing end signal intensities, the polymer was equally prehydrolyzed for all experiments at 95 °C (pH 5.6 for 3.5 h) to a number-average DP between 30 and 50, constituting the initial (0 h) NMR spectrum in Figure 5. Characteristic resonance signals from the reducing ends could thus be obtained from just 1.5 h degradation time (see Figure 5), even if the accurate integration of M reducing end signal intensities was not as good

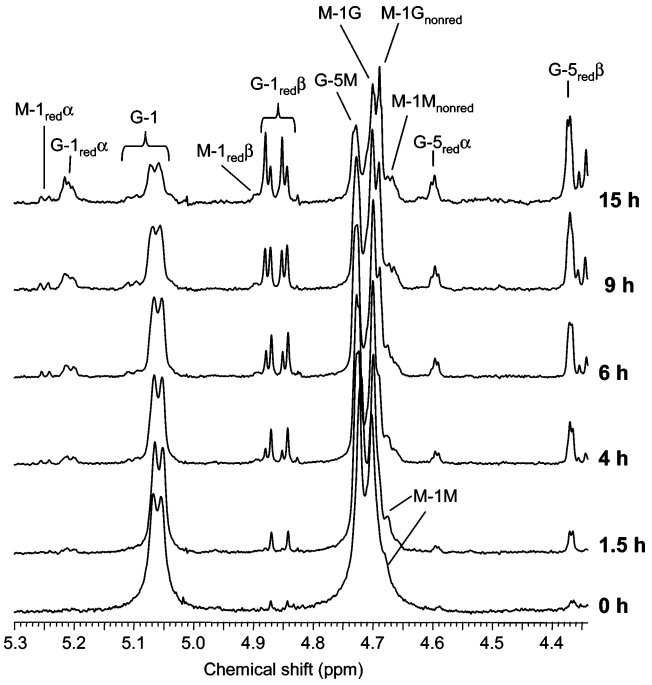

Figure 5. ^{1}H NMR (300 MHz) spectra of PolyMG from start (0 h) and after 1.5, 4, 6, 9, and 15 h hydrolysis time at pH 3.5 and 95 °C. The prefixes "red and nonred", respectively denote the reducing and nonreducing ends increasing in signal intensities by hydrolysis time.

as those of the G reducing end. From the NMR spectra in Figure 5, a split of the G-1$_{red}\beta$ resonance signal at 4.86 ppm with the same spin coupling constant ($J_{1,2} = 8.3$ Hz) can be seen from 1.5 h degradation time, increasing in intensity and after 9 h (DP_n of 4.9) being the most dominant G-1$_{red}\beta$ resonance signal. This new doublet peak is due to β-anomeric G reducing ends of dimers (MG) most prominent or monomers (low stability) in the hydrolysate. Compared to the NMR spectra in Figure 3 recorded at p^{2}H 4.0, the peaks assigned to H-5 of G residues, namely G-5M, G-5$_{red}\alpha$, and G-5$_{red}\beta$, have moved upfield in the spectra of Figure 5 recorded at p^{2}H 5.5, proving their p^{2}H dependency due to the close vicinity to the C-5 carboxyl group as reported by Grasdalen.[20,27] Upfield shifts can also be observed for the M-1G and M-1M signals by increasing hydrolysis time (see Figure 5), due to the appearances of less deshielded anomeric M nonreducing end resonance signals.

From the ^{1}H NMR spectra using the similar reducing end signals for G and M as described above (the G-5$_{red}\alpha$ signal arises at 4.59 ppm for p^{2}H 5.5), α_G and α_M were calculated for the time series at each pH value. The rate constants k_{G-M} and k_{M-G} for each acidity were found by plotting $-\ln(1-\alpha)$ for calculated values of α_G and α_M, as a function of time. Straight lines were obtained for degradation of both G−M and M−G linkages at every pH examined, shown for pH 3.5 in Figure 6. To avoid any influence from ends on the degradation rates, hydrolysis times giving $DP_n > 4$ of hydrolysates were used for calculations. From the ^{1}H NMR monitored hydrolysis experiment, linearity was confirmed until a DP_n of 4.2. For pH 3.5 in Figure 6, the calculations of respective rate constants were based on hydrolysis up to 9 h and a number-average DP of 4.9 of the hydrolysate, ensuring that the β-anomeric G signals from oligomers with DP > 2 were dominant (Figure 5). The specific hydrolysis rates expressed as the slope of the curves for all four pH values are given in Table 1. At pH 3.5, the ratio of the rate constants, k_{G-M}/k_{M-G}, was 10.7.

As for the NMR-monitored acid hydrolysis of PolyMG at p^{2}H 4.0, the plotting of results for separately hydrolyzed samples

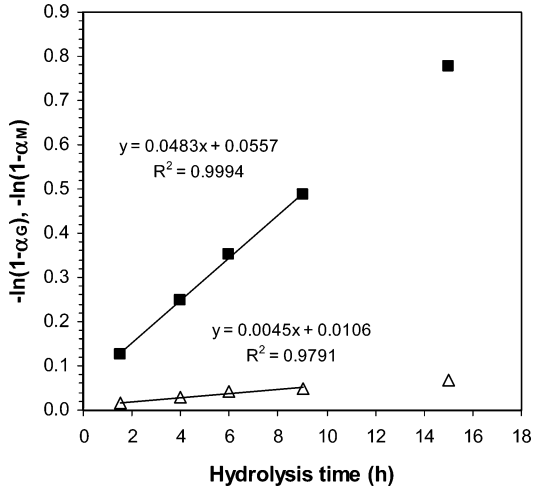

Figure 6. Rate of degradation of G−M (■) and M−G (△) glycosidic linkages in PolyMG at pH 3.5 and 95 °C. The respective rate constants, k_{G-M} (■) and k_{M-G} (△), were determined from the slope of the curves up to 9 h degradation time and a number-average DP of 4.9 of the hydrolysate.

at pH 3.5 according to first-order reactions gave a better linearity for G−M than M−G degradation rates (Figures 4 and 6). In addition to inaccuracy in peak integration of NMR signals explaining the poorer regression fit for k_{M-G} than k_{G-M} (see previous section), the extra 6% MM content in PolyMG with 47% G involves an additional linkage M−M, which by cleavage influences the amount of M at the reducing end in the hydrolysis reaction, and thus k_{M-G}. Changing the residue linked to M-4 of an M reducing end will affect the chemical shift,[11] here only observable for the anomeric α signal. The MM-1_{red}α resonates at 5.21 ppm and constitutes one of the additional peaks overlapping with the G-1_{red}α signal (see Figures 3 and 5). In present work, only the GM-1_{red}α signal was used for calculation of F_{Mred}. Cleavage of M−G linkages following an M-block or M−M linkages in M blocks consisting of more than two residues both generating MM reducing ends would therefore not be counted. However, degradation of M−M linkages in the polymer chain leading to GM reducing ends could influence the calculation and linearity of the k_{M-G} curve. The degradation rate of mannuronan ($F_M = 1.0$) was therefore examined under the same conditions at pH 3.5. The rate constant k_{M-M} was of first order designating random degradation of mannuronan. M−M linkages were hydrolyzed at an intermediate rate compared to G−M and M−G linkages in the polymer, see Table 1. The ratio k_{M-M}/k_{M-G} was 2.8, indicating that the minor influence from M−M cleavages in this study taken into consideration would give a small underestimation of the measured ratio of G−M to M−G degradation rates. On the other hand, considering the prehydrolysis of PolyMG to a DP_n between 30 and 50 prior to the kinetic experiments at different acidities (including pH 3.5), the examined faster degradation rate of M−M than M−G linkages would lead to more M−M than M−G cleavages. The average M block length ($N_{M>1}$) of PolyMG with $DP_n \approx 30$ was calculated to approximately 2 by ^{13}C NMR (Figure 2). Because of this, the contribution from M−M degradation on the calculation of k_{M-G} is reduced even more in this study.

In a parallel study using the same starting PolyMG ($F_G = 0.47$), similar conditions of partial hydrolysis at pH 3.6 and a statistical analysis based on HPAEC−PAD experimental data of the weight distribution of chain lengths in the hydrolysate to determine the ratio of k_{G-M} to k_{M-G}, a value of 8.3 ± 1 was obtained.[23] The block length and distribution of the 6% extra

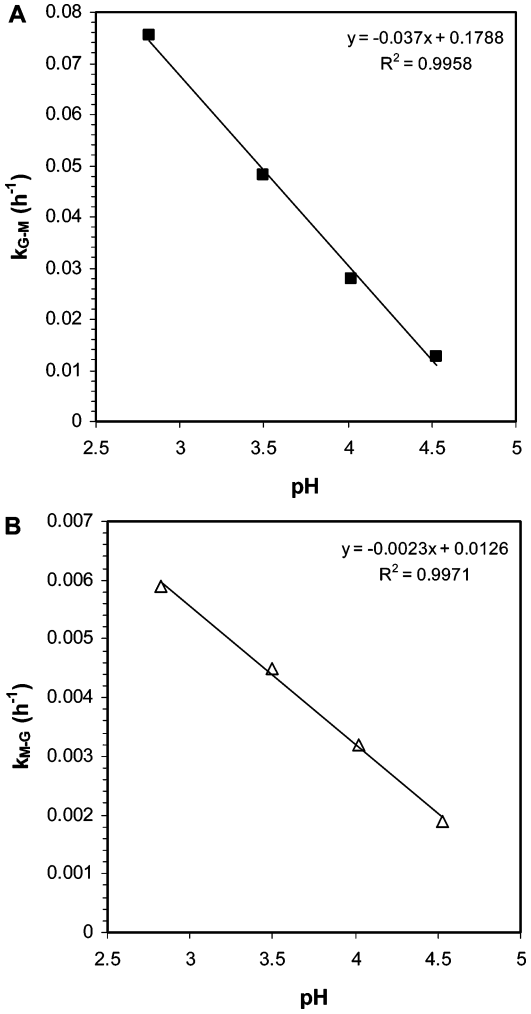

Figure 7. The pH dependency of the rate constants (A) k_{G-M} and (B) k_{M-G} in the pH range of 2.8−4.5.

M units in the polymer were taken into account for this calculation. This value is in good agreement with the ratio of the rate constants of 10.7 at pH 3.5 measured here directly by ^{1}H NMR.

The pH dependence of the rate constants k_{G-M} and k_{M-G} and the ratio k_{G-M} to k_{M-G} is shown in Table 1 and graphically in Figure 7. Both curves of the respective rate constants against pH in Figure 7 display good fits to linearity within the small pH− range examined. An increase in pH from 2.8 to 4.5 gives approximately 16 times greater decrease in k_{G-M} than k_{M-G}, thus leading to a decrease in the ratio of these rate constants by increasing pH. This is evidence of an intramolecular catalyzed cleavage of the glycosidic linkages by the undissociated carboxyl groups acting directly as proton donors as suggested by Smidsrød et al.[16] The →4)-α-L-Gul*p*A-(1→4)-*β*-D-Man*p*A-(1→ linkages in the PolyMG chain are more rapidly protonated and hydrolyzed than the →4)-*β*-D-Man*p*A-(1→4)-α-L-Gul*p*A-(1→ linkages. In the G−M linkages, the positioned carboxyl groups at C-5 of the mannuronic acid residues are stabilized by intramolecular hydrogen bonds to the hydroxyl groups of carbon atoms 2 and 3 in the preceding guluronic acid residues. The greater decrease in k_{G-M} than k_{M-G} in the pH range 2.8−4.5 reflects the difference in pK_a values for mannuronic and guluronic acid residues.[26] Because of the more dissociated carboxyl groups of mannuronic acid residues, the cleavage of the G−M glycosidic linkages is affected more than the M−G linkages by increasing the pH to 4.5. The less stabilization of carboxyl groups at C-5 for guluronate, for catalysis of cleavage

of the glycosidic linkage entering C-4 of the same residue could increase the contribution from proton-catalyzed hydrolysis of M−G linkages. Hydrolysis of PolyMG under the same conditions at pH 3.5 but with the addition of 0.15 M NaCl was performed, and the degradation rates are given in Table 1. This increase in ionic strength lowered the degradation rate for both G−M and M−G linkages. The shielding of carboxyl groups and decrease in k_{G-M} are the most notable, leading to a slight decrease in the ratio of the two rate constants compared to degradation without salt. This result confirms that intramolecular catalysis is the dominant mechanism for cleavage of the two types of glycosidic linkages in PolyMG at pH 3.5.

The respective rate constants from acid hydrolysis of PolyMG performed in the NMR spectrometer at p^{2}H 4.0 (corresponding to pH 4.4)[24] and 95 °C were compared with the rate constants from degradation at pH 4.5 (being closest to pH 4.4) and 95 °C. From Table 1, it can be seen that the degradation rate for G−M linkages is 3 times higher in weak ^{2}HCl than in HCl, whereas the ratio of k_{M-G} in weak ^{2}HCl to HCl is 1.3, enhancing the ratio between the rate constants k_{G-M} and k_{M-G} to 15.6 in ^{2}HCl against 6.7 for the degradation in HCl. This is in agreement with previously reported higher rates of hydrolysis of sugars in ^2H_2O, and within the order of most of the accelerations of 1.3−3.0 for the use of ^2H_2O as solvent in acid-catalyzed reactions in general.[28] The concentration of the conjugate acid of the glycoside (G-^{2}H$^+$) will be higher in ^2H_2O than in H_2O, due to a smaller dissociation constant of the deuteron acid than the proton acid affecting step two and the formation of a carbocation, which is the rate-limiting step in the mechanism for acid hydrolysis.[29,30] The autoprotolysis constant of ^2H_2O is in addition smaller than of H_2O, affecting the protonation and formation of the labile conjugate acid (step one), together with the last step of the acid hydrolysis.[28] This suggests that the observed higher rates of degradation in weak deuteron acid at p^{2}H 4.0 compared to weak proton acid are mainly due to a greater contribution from ^{2}H$^+$-catalyzed hydrolysis as mechanism for glycosidic cleavage, especially for the G−M linkages.

The rate of degradation of PolyMG at a polymer level (k_{PolyMG}), considering both glycosidic linkages, was calculated from the equation, $k = k_{G-M}F_G + k_{M-G}F_M$, using the specific rate constants k_{G-M} and k_{M-G} and the mole fractions of mannuronic and guluronic acid residues. The k values for all examined acidities are shown in Table 1. The contribution of the extra 6% mannuronic acid content in PolyMG forming M−M linkages degraded at a higher rate than M−G linkages was determined at pH 3.5 to constitute only 0.4% deviation of the calculated value for k and was therefore not taken into account. For pH 2.8 and 3.5, the calculated k values are compared with previously reported values[16] for degradation of oligomers ($DP_n \approx 20$) enriched in alternating sequences (60% M). Measuring the increase in reducing power with time and plotting the results according to first order kinetics gave the rate constants of 0.055 (pH 2.8) and 0.025 (pH 3.6) from the initial slope of the curves. The slightly higher k values in Smidsrød et al.[16] for degradation at equal acidities have a number of explanations. Because of nonrandom degradation and a higher M content of the starting material than PolyMG, the initial k value represents a combination of k_{G-M} and k_{M-M}, together with k_{M-G} though minor. The degradation rate of mannuronan at pH 3.5 given in Table 1 is much lower than k_{M-M} reported to be 0.035 at pH 3.6 by Smidsrød et al.[16] The difference in DP_n of the starting material of 5[16] to close to 50 in this study and reduced contribution from the chains ends on the degradation rate can explain this discrepancy. The rate of hydrolysis of alginates is hereby shown to be dependent both on the composition and the distribution of mannuronic and guluronic acid residues along the chain, the intramolecular catalyzed cleavage of the G−M glycosidic linkages being dominant to M−M and M−G linkages at weak acidities.

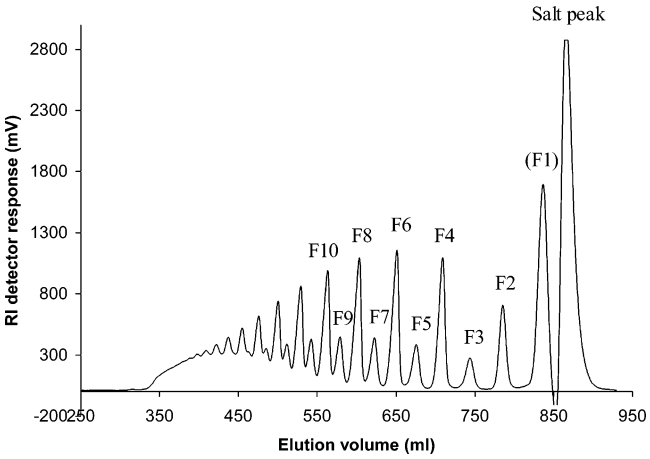

Figure 8. Preparative Superdex 30 chromatography of a 4 h partially hydrolyzed PolyMG ($F_G = 0.47$) eluted with 0.1 M NH_4Ac at a flow rate of 0.8 mL min^{-1}. The eluent was monitored on-line with a refractive index detector.

Preparation of MG Oligomers. The higher degradation rate in weak acids of G−M than M−G glycosidic linkages in the polymer chain of MG-alginate was exploited to make oligomers mainly consisting of M on the nonreducing and G on the reducing end and, thus, a majority of oligomers with an even number of residues. A large batch of PolyMG ($F_G = 0.47$) was hydrolyzed at pH 3.5 in an identical manner to that described above, for 4 h to a number-average DP of 7 as determined by ^{1}H NMR of the resulting hydrolysate. The respective rate constants k_{G-M} and k_{M-G} were found by using the equation $-\ln(1-\alpha) = kt$, for calculated values of α_G and α_M from ^{1}H NMR and t equal to 4 h. The ratio of the rates k_{G-M}/k_{M-G} was 10.4. This result is in good agreement with the ratio of 10.7 at pH 3.5 obtained by the kinetic experiment.

SEC of the MG-hydrolysate on Superdex 30 yielded a series of distinct and well-resolved peaks (Figure 8). Excluding the salt peak, 16 distinct peaks were resolved with areas roughly representative of the amounts of respective fractions. Each peak (F2−F16) was presumed to represent pure oligomer with a chain length from 2 to 16 uronic acid residues consecutively, with only negligible contributions from homologues one monomer unit apart. The monomer fraction (F1), however, was not studied further because it coeluted with the NH_4Ac− salt peak. Figure 8 clearly indicates that the even numbered fractions are far larger than the odd numbered fractions (except for F1). This difference in peak areas is thus reflecting the excess generation of oligomers with an even number of residues namely with an M on the nonreducing and a G on the reducing end as a consequence of the ratio of the degradation rates k_{G-M}/k_{M-G} of 10.4. The DP_n of 7 of the MG-hydrolysate yielded the most eluted material in fraction 6 accounting for 7.3% of the total injected material followed by fractions 4 and 8, which were equal in size and accounted for 6.9% of the injected material. In comparison, the odd fractions 5, 7, and 9 were 2.5 times smaller and accounted for less than 3% of total. The monomer fraction (F1) was included in these calculations, and considering the coelution of NH_4Ac in this fraction, the relative amounts of the other oligosaccharide fractions were somewhat higher (F6 constituted 8.6% of total material minus F1).

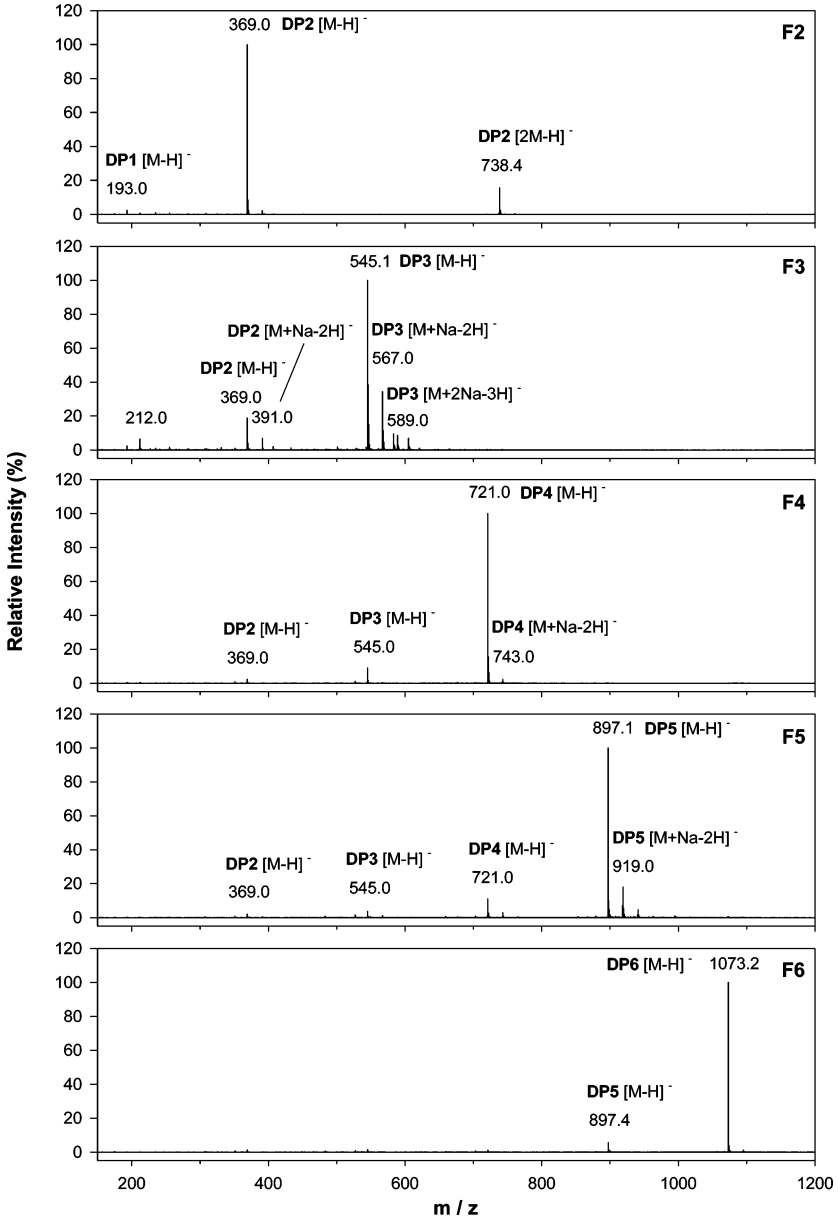

Figure 9. Negative-ion ESI mass spectra of oligouronic acid fractions 2−6 obtained from a 4 h partial hydrolysis of PolyMG ($F_G = 0.47$) followed by separation by SEC on Superdex 30. DP and the respective integer (1−6) refers to the degree of oligomer polymerization. Capillary voltage: 3.5 kV; solvent: aqueous 50% CH_3OH containing 1% NH_3.

Since two first-order rate constants and random degradations of G−M and M−G glycosidic linkages in PolyMG when considered separately were determined, the calculated values of α_G and α_M from ^{1}H NMR of MG-hydrolysate could be used to calculate the expected weight fractions of the various oligomers by using the equation $W_n = n\alpha^2(1-\alpha)^{n-1}$. However, these calculations gave a greater difference in weight ratio between even and odd numbered fractions than found by SEC (data not shown). The 6% extra MM content in PolyMG distributed in short blocks and that k_{M-M} was determined to be larger than k_{M-G} were therefore considered to imply an influence on the weight distribution of chain lengths in the hydrolysate, as shown in Ballance et al.[23] This could happen either by increasing the rate by which oligomers with an odd number of residues are made itself or by making up irregularities in the chains which are shifting the degradation pattern such that two rapid G−M cleavages lead to odd numbered oligomers as well as even ones. As discussed in a previous section, the contribution from M−M degradation on the calculation of α_M is minimized in this study.

ESI-MS Analysis. The negative-ion mode mass spectra of fractions 2−6 displayed signals attributable to the main deprotonated oligomers $[M-H]^-$ (where M is the main solute molecule) and ions with Na $[M+Na\text{-}2H]^-$ (Figure 9). The most abundant oligomer in the fractions corresponds to the most abundant deprotonated ion, such as that at *m*/*z* 721.0 (DP4) in F4. Also, in the same fraction, lower homologues are present at *m*/*z* 369.0 (DP2) and 545.0 (DP3), with the former present in only trace amounts (Figure 9). Similar results were obtained for fractions 2, 3, 5, and 6. However, the amount of lower homologues and ions with Na was higher in the odd numbered fractions (Figure 9). Mass spectra of fractions 7−16 were more complex due to an increase in double-charging phenomena. Analysis of the mass spectra of the same fractions F2− F16 in the positive-ion mode was more sensitive, but even more complex (spectra not shown), because of a greater amount of ion adduction.

Assignment of NMR Spectra of MG Oligomers. Due to the high salt concentration in fraction one and the low stability of the monomer, the NMR analysis was carried out from fraction

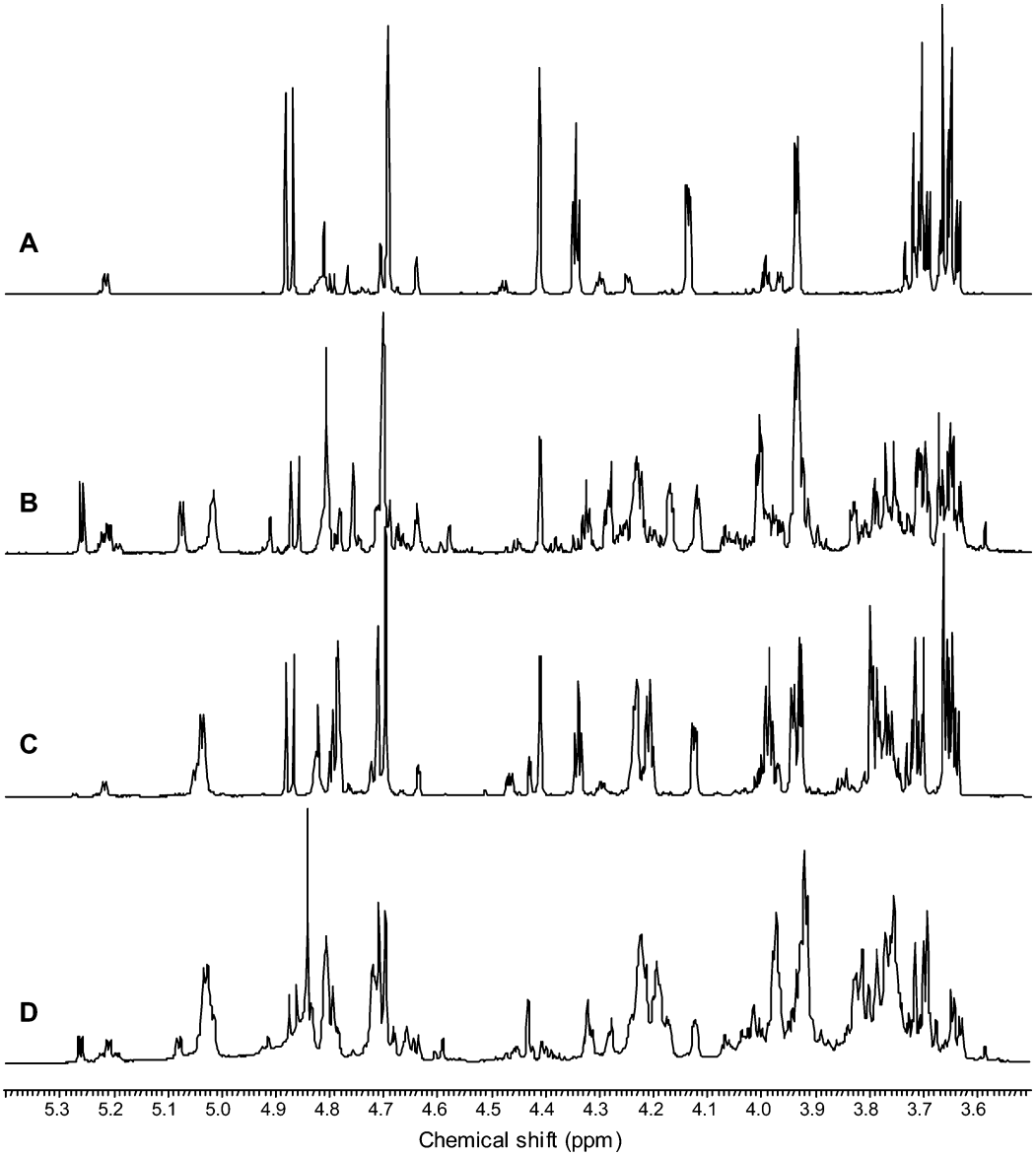

Figure 10. ^{1}H NMR (600.1 MHz) spectra of (A) dimer, (B) trimer, (C) tetramer and (D) pentamer. The experimental temperature was 298 K for panels A−C and 295 K for panel D. The p^{2}H of the samples was 4.5 ± 0.3.

two. Upward fraction two exhibits a very clean ESI-MS spectrum with a molecular mass corresponding to dimer. The ^{1}H and ^{13}C NMR spectra for fraction two were recorded on a Bruker Avance 600 spectrometer at room temperature and are shown in Figures 10A and 11A, respectively. To assign peaks in ^{1}H and ^{13}C NMR spectra, ^{1}H−^{1}H COSY, ^{1}H−^{13}C HSQC, and ^{1}H−^{13}C HMBC 2D NMR experiments were carried out (Figure 12). The resonance signals from anomeric protons were easily assigned according to previous data for alginate polymers and oligomers.[20,22,31] The peak at 5.21 ppm is assigned to the resonance of the reducing end G-1$_{red}\alpha$ with a proton coupling constant $J_{1,2}$ of 3.4 Hz and a typical ^{13}C−^{1}H spin coupling constant $J_{C-1,\ H-1}$ of 171 Hz from the HMBC spectrum. The proton signal at 4.87 ppm is from the reducing end G-1$_{red}\beta$, with a proton coupling constant $J_{1,2}$ of 8.6 Hz and ^{13}C−^{1}H coupling constant $J_{C-1,\ H-1}$ of 162 Hz. From the HSQC spectrum, the resonance signals from anomeric carbons at the G reducing end appear at 96.02 ppm in a β configuration and 95.86 ppm in a α configuration. Starting from the anomeric proton signals from the reducing ends, other proton signals from the reducing ends of dimers were identified with the cross-peaks in the ^{1}H−^{1}H COSY 2D NMR spectrum. Furthermore, the corresponding ^{13}C signals were also assigned by ^{1}H−^{13}C HSQC NMR spectra. The chemical shift values of ^{1}H and ^{13}C peaks are given in Table 2. From the cross-peak between the number four atom H-4 (or C-4) on the reducing end and the anomeric atom C-1 (or H-1) on the neighboring nonreducing end in the HMBC NMR spectrum (Figure 12), the glycosidic linkage between a reducing end and a nonreducing end was identified. The chemical shift values for nonreducing ends are given in Table 2. The signals from the M reducing end for the GM dimer are at such a low level that they are negligible in fraction 2; that is, most dimers have M on the nonreducing end and G on the reducing end. This is consistent with the faster cleavage of G−M than M−G glycosidic linkages as explained in previous sections. From the integration of anomeric signals of the G reducing end in the ^{1}H NMR spectrum, a quantitative ratio of G$_{red}\alpha$ to G$_{red}\beta$ is determined as 0.21. On the other hand, for the MM dimer which is also a possible component in this fraction, the corresponding α anomeric signal of the M reducing end is expected to appear near the proton signal of G-1$_{red}\alpha$ according to our result,[11] indicated by a low and shallow shoulder on the left of the G-1$_{red}\alpha$ doublet. The signals from MM dimers are not considered here due to their much lower intensity.

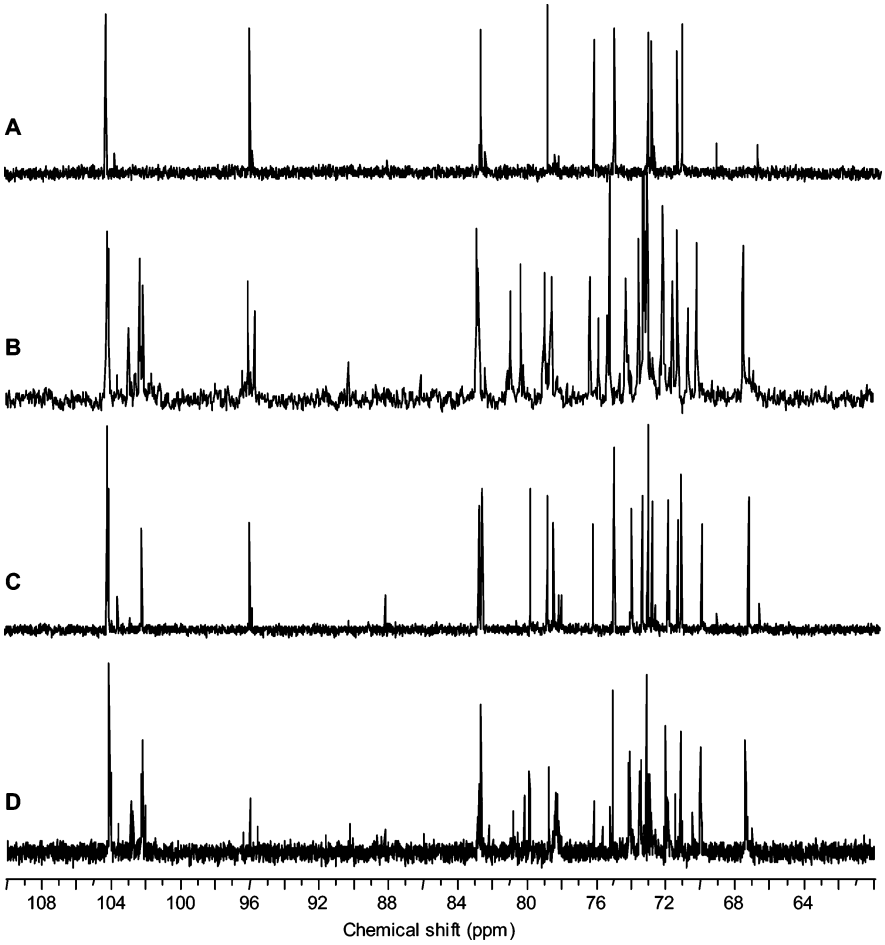

Figure 11. ^{13}C NMR (150.9 MHz) spectra of (A) dimer, (B) trimer, (C) tetramer, and (D) pentamer. The experimental temperature was 298 K for panels A−C and 295 K for panel D. The p^2H of the samples was 4.5 ± 0.3.

Compared to fraction 2, fraction 3 exhibits more complicated ^1H and ^{13}C NMR spectra as shown in Figures 10B and 11B, respectively. The $^1H-^1H$ COSY, $^1H-^{13}C$ HSQC, and $^1H-^{13}C$ HMBC 2D NMR spectra of the trimer are shown in Figure 13. The resonance signals from anomeric protons of reducing ends at 5.26 ppm for M-$1_{red}\alpha$, 4.91 ppm for M-$1_{red}\beta$, 4.87 ppm for G-$1_{red}\beta$, and 5.21 ppm for G-$1_{red}\alpha$ were identified in the ^1H NMR spectrum according to previous work. Using the same procedure as for the dimer, i.e., from the identified anomeric signals of the reducing ends, both ^1H and ^{13}C peaks from the reducing ends were assigned by $^1H-^1H$ COSY 2D NMR spectrum and $^{13}C-^1H$ HSQC 2D NMR spectrum. The anomeric signals from the residues preceding each form of reducing end were identified by the cross-peaks between their H-1 atom and the C-4 atom of the reducing ends, followed by identification of all of the ^1H and ^{13}C signals of the internal residues. The nonreducing ends corresponding to each of the trimers were identified by the cross-peaks arisen from their anomeric atom and the number four atom of the internal residues. From the integration of anomeric signals from the MGM reducing end in the ^1H NMR spectrum, a quantitative ratio of $M_{red}\alpha$ to $M_{red}\beta$ is determined as 2.0. The chemical shift values of ^{13}C and ^1H for the trimers in fraction 3 are shown in Table 2. The $^1H-^1H$ TOCSY 2D NMR spectrum was used to reconfirm the resonance signals from the same residues (spectrum not shown).

1D and 2D NMR spectra were also recorded for fractions 4 and 5 (see Figures 10 and 11 for 1D spectra; 2D spectra are not shown). The ^{13}C and ^1H chemical shift values are shown in Table 2. For the tetramer as for the dimer, mainly G residues appear on the reducing ends. More than 90% G of total reducing ends were determined for both oligosaccharide fractions by integration of the signal intensities in the spectra in Figure 10. In contrast, both G and M reducing ends are observed in the pentamer, which is similar to the trimer. This is caused by the mechanism of hydrolysis described in previous sections. Whereas two rapid G−M cleavages lead to oligomers with an even number of residues, an additional slower M−G cleavage to a G−M cleavage is needed for the generation of odd numbered ones. This implies that approximately 50% of the odd numbered oligomers will have an M residue on the reducing end. Integration of the signal intensities from the reducing ends for the trimer and pentamer in the spectra in Figure 10 gave a total of approximately 45% M reducing ends. However, the higher amount of lower homologues in the odd numbered oligomers determined by ESI-MS (Figure 9) could contribute to the observed little excess of G reducing ends, stemming from even numbered oligomers minus one monomer residue in chain length. As mentioned before, the 6% extra MM content in PolyMG distributed in short blocks and the fact that k_{M-M} is larger than k_{M-G} suggest that the irregular sequences will be found in the low molecular mass fractions after hydrolysis. The signal intensity of MM-$1_{red}\alpha$ was not included in the calculations of the amount of M and G reducing end signal intensities in the fractions above, such that only GM and MG reducing ends were taken into account. For the trimer fraction, the resonance signals at approximately 4.68 ppm in the ^1H NMR spectrum in Figure 10B are attributed to internal and/or nonreducing end M-1M. Likewise, the resonance signals at 103 ppm in the ^{13}C NMR spectrum of the trimer in Figure 11B are most likely attributed to M<u>M</u>M (G<u>M</u>M) sequences in the sample. The

Table 2. ^{1}H and ^{13}C NMR Chemical Shifts of Oligomers Obtained by Acid Hydrolysis of PolyMG[a]

	proton chemical shifts (ppm)					carbon chemical shifts (ppm)				
	H-1	H-2	H-3	H-4	H-5	C-1	C-2	C-3	C-4	C-5
MG dimer										
$\underline{MG}_{red\beta}$	4.87	3.69	4.34	4.13	4.41	96.02	71.62	73.10	82.87	76.52
$\underline{MG}_{red\beta}$	4.69	3.93	3.64	3.65	3.71	104.23	73.30	75.20	79.01	71.36
$\underline{MG}_{red\alpha}$	5.21	3.99	4.29	4.24	4.63	95.86	67.01	72.91	82.95	69.41
$\underline{MG}_{red\alpha}$	4.70	3.93	3.64	3.65	3.71	104.19	73.31	75.22	79.01	71.36
GMG trimer										
$GMG_{red\beta}$	4.87	3.70	4.33	4.12	4.40	96.03	71.57	73.06	82.86	76.34
$G\underline{MG}_{red\beta}$	4.70	3.93	3.75	3.77	3.79	104.07	73.14	74.26	80.31	78.53
$GMG_{red\alpha}$	5.21	4.07	4.26	4.24	4.64	95.88	67.16	72.70	82.89	69.31
$G\underline{MG}_{red\alpha}$	4.70	3.93	3.75	3.77	3.79	104.07	73.14	74.26	80.31	78.53
$\underline{GMG}$	5.02	3.93	3.94	4.17	4.76	102.29	67.51	73.25	73.53	70.70
MGM trimer										
$MGM_{red\beta}$	4.91	3.91	3.77			96.40	73.98	74.65		
$\underline{MGM}_{red\beta}$	5.02	3.98	4.20	4.22	4.78	102.08	67.51	72.12	82.69	70.18
$MGM_{red\alpha}$	5.26	3.83	4.00	4.00	4.29	95.66	73.03	72.12	80.90	75.84
$\underline{MGM}_{red\alpha}$	5.07	4.00	4.23	4.24	4.70	102.08	67.47	72.12	82.78	70.18
$\underline{MGM}$	4.70	3.93	3.64	3.66	3.71	104.17	73.03	75.84	79.03	71.31
MGMG tetramer										
$MGMG_{red\beta}$	4.87	3.70	4.33	4.12	4.40	96.01	71.57	73.02	82.92	76.39
$MG\underline{MG}_{red\beta}$	4.70	3.93	3.75	3.79	3.74	104.08	73.59	74.20	79.97	78.66
$\underline{MGMG}_{red\beta}$	5.03	3.98	4.20	4.22	4.78	102.17	67.52	72.20	82.75	70.20
$MGMG_{red\alpha}$	5.21	4.00	4.29	4.23	4.63	95.88	66.91	72.87	82.98	69.35
$MG\underline{MG}_{red\alpha}$	4.71	3.93	3.75	3.79	3.74	104.04	73.59	74.27	79.95	78.66
$\underline{MGMG}_{red\alpha}$	5.04	3.98	4.21	4.23	4.79	102.20	67.52	72.22	82.72	70.20
$\underline{MGMG}$	4.69	3.92	3.64	3.65	3.71	104.13	73.25	75.20	79.01	71.35
GMGMG pentamer										
$GMGMG_{red\beta}$	4.86	3.69	4.32	4.12	4.43	96.02	71.51	73.07	82.89	76.22
$GMG\underline{MG}_{red\beta}$	4.72	3.91	3.75	3.79	3.74	104.02	73.57	74.20	79.89	78.41
$GMGMG_{red\alpha}$	5.21	4.07	4.24	4.28	4.68	95.85	67.07	72.16	82.27	69.99
$GMG\underline{MG}_{red\alpha}$	4.70	3.91	3.75	3.79	3.74	104.12	73.57	74.20	79.89	78.46
$GMG\underline{MG}$	5.03	3.97	4.19	4.22	4.80	102.21	67.46	72.06	82.71	70.07
$GMG\underline{MG}$	4.70	3.91	3.75	3.79	3.74	104.12	73.18	74.14	79.91	78.33
$\underline{GMGMG}$	5.02	3.93	3.94	4.17	4.79	102.27	67.42	73.18	73.54	70.54
MGMGM pentamer										
$MGMGM_{red\beta}$	4.91	3.91				96.41	72.91			
$MGMG\underline{M}_{red\beta}$	5.03	3.97	4.19	4.22	4.80	102.27	67.46	72.06	82.71	70.07
$MGMGM_{red\alpha}$	5.26	3.82	4.01	4.31	4.01	95.58	72.97	72.12	80.88	75.71
$MGMG\underline{M}_{red\alpha}$	5.08	4.00				102.21	67.40			
$MG\underline{MG}M$	4.70	3.91	3.75	3.79	3.74	104.12	73.18	74.14	79.91	78.33
$MG\underline{MG}M$	5.03	3.97	4.19	4.22	4.80	102.21	67.46	72.06	82.71	70.07
$\underline{MGMGM}$	4.69	3.91	3.64	3.66	3.71	104.17	73.18	75.13	78.79	71.21

[a] The observed residue was indicated with an underline. The p^2H of the samples was 4.5 ± 0.3.

identification of $^{1}H-^{13}C$ cross-peaks in the HSQC spectrum (Figure 13B) confirmed the presence of trimers with irregular structures. The similar resonance signals are also observed for the pentamer fraction. The more clean NMR spectra for the even numbered oligomers lacking additional peaks at 4.68 ppm for ^{1}H and 103 ppm for ^{13}C and a low percentage of M reducing ends indicates that after hydrolysis most irregular sequences are found in the oligomers with an odd number of residues and low DP. Even though a little contribution to the MG reducing end signal intensity from pollution of the odd numbered fractions with even ones, a lower signal intensity of GM reducing ends than expected (<50%) suggests a minimal contribution from MM dimer degradation to the GM reducing end intensity. Consequently and proved by the internal irregular NMR signals for the odd fractions, the extra M content in PolyMG (F_G = 0.47) with the dimer (MM) fraction as most abundant is shifting the degradation pattern at specific points of the chain such that two rapid G−M cleavages here lead to odd numbered oligomers with irregularities, i.e., MG↓MGMMG↓M for the pentamer. This is in agreement with the weight distribution of chain lengths in the hydrolysate found by SEC and larger odd numbered fractions than expected when calculated from the ^{1}H NMR measured degree of scission of G−M and M−G linkages (see the previous section).

Peaks Overlapping the α Anomeric Peak of the G Reducing End. In the ^{1}H NMR spectrum of the trimer (Figure 10B) and pentamer (Figure 10D), extra weak doublets are clearly distinguished due to the high resolution spectrum obtained at higher field. To our knowledge, it is the first time the heavily overlapped peaks near the α anomeric peak of the G reducing end are given any attention. The ESI-MS analysis of the oligosaccharide fractions excludes the possibility that these signals are due to contamination, and they are further found in oligomers from hydrolysis of both bacterial and algal alginate. The proton signal intensity of G-$5_{red}\alpha$ was therefore chosen instead of G-$1_{red}\alpha$ for quantitative calculation in the kinetic study in the previous section. As discussed for the dimer, the α anomeric resonance signal of irregular MM reducing ends appears near the G-$1_{red}\alpha$ peaks,[11] and for the odd numbered fractions in particular it is very likely that parts of the extra

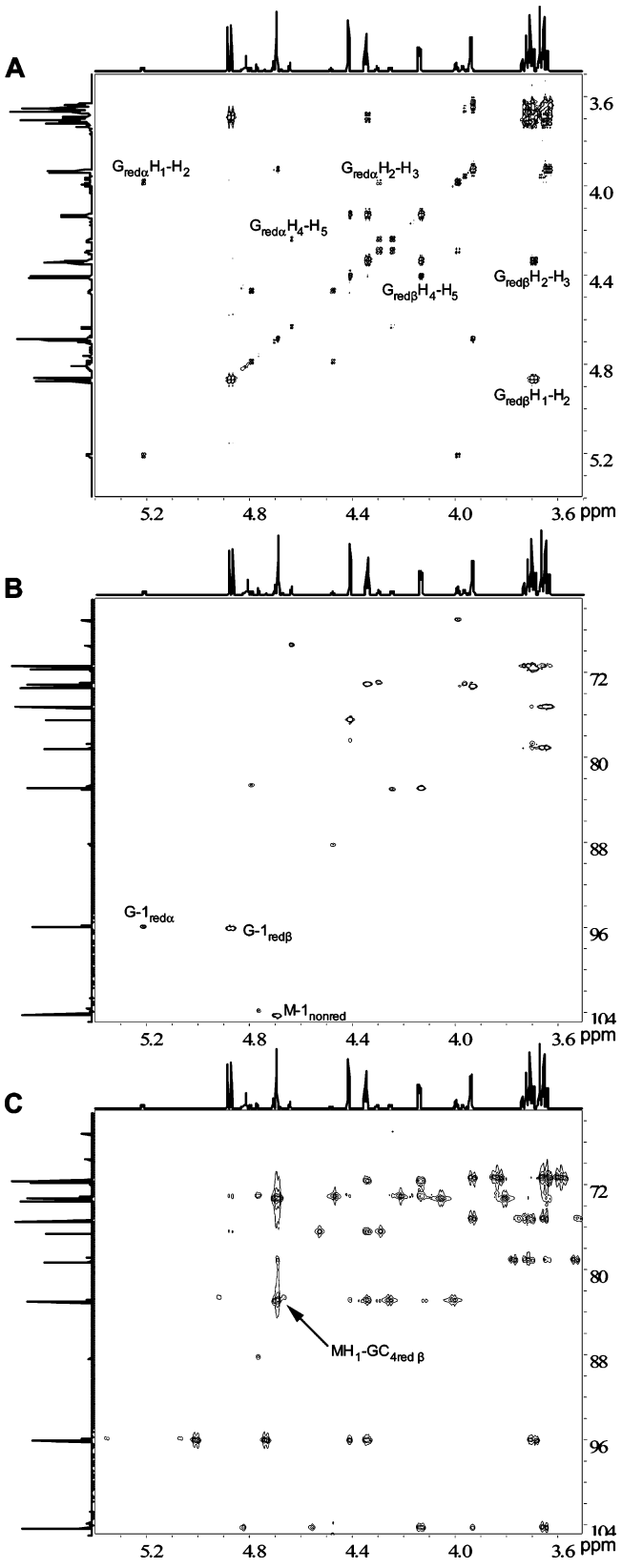

Figure 12. 2D NMR spectra of dimer obtained at p^{2}H 4.5 and room temperature. (A) COSY, (B) HSQC, and (C) HMBC.

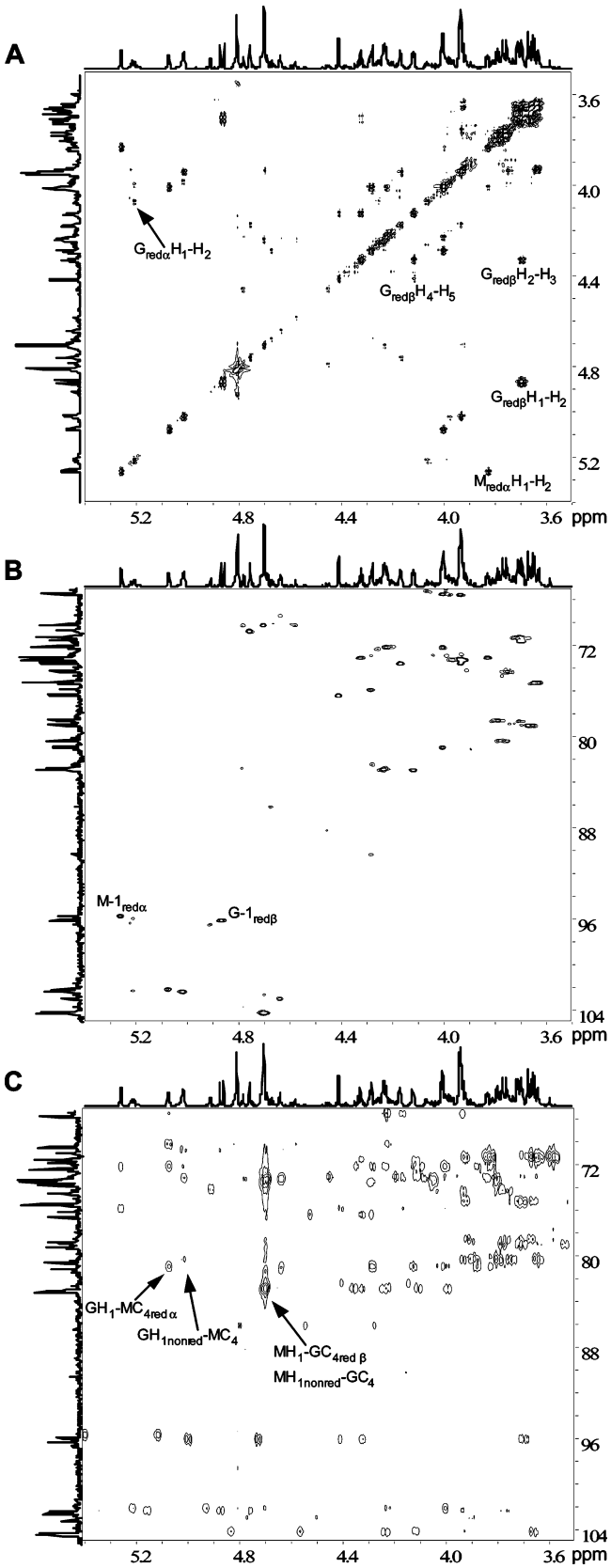

Figure 13. 2D NMR spectra of trimer obtained at p^{2}H 4.5 and room temperature. (A) COSY, (B) HSQC, and (C) HMBC.

peaks arise from irregular MMM and/or GMM sequences as discussed above. Moreover, since these series of weak doublets were most apparent and observed in all of the spectra recorded for oligomers with an odd number of residues decreasing in intensity with increasing DP of samples (more present in the trimer than pentamer), the higher amount of M reducing and G nonreducing ends in these samples compared to the even numbered ones were taken into consideration. By increasing the temperature for the ^{1}H NMR experiments from 25 to 90 °C, an increase in signal intensities of the G-$1_{red}\alpha$ overlapping peaks was observed. This suggests their origin is from confor-

mational changes, presumably occurring at the reducing ends of oligomers with low DP.[32] In the ESI mass spectra (Figure 9), small signals at *m*/*z* 501.0 and 527.0 for the trimer (F3) and at *m*/*z* 853.0 and 879.1 for the pentamer (F5) were attributable to degradation by decarboxylation[29] and loss of water, respectively. Although these signals might occur by fragmentation during the MS analysis, their absence in the dimer (F2), tetramer (F4), and hexamer (F6) fraction suggests that the odd numbered fractions undergo a more rapid dehydration and decarboxylation. To examine this further, the p^{2}H of the samples was raised to 8.5 and ^{1}H NMR spectra were recorded at room temperature. The weak doublet peaks showed no displacement (spectra not shown), excluding the possibility of a γ- or δ-lactone structure that may arise from the β-D-mannuronic acid residues at the reducing ends by reconfiguration during acid hydrolysis. On the other hand, we found that some additional peaks in the ^{1}H NMR spectra became a little stronger by storage (spectra not shown), suggesting that the extra doublets are a result of the lower stability of the M (mainly in their α form) than G reducing ends and an acid-catalyzed modification of the reducing ends of the oligosaccharides, mainly by storage in their H^+ form. We believe this is the most likely explanation for these series of weak doublets, but more experimental evidence is required in order to elucidate the chemical structure they represent.

Conclusion

The availability of mannuronan C-5 epimerase AlgE4 enables the production of a strictly alternating alginate (PolyMG) with $F_G = 0.47$ and $F_{GG} = 0.0$, chiefly consisting of two types of (1→ 4)-glycosidic linkages susceptible for hydrolysis; α-L-Gul*p*A-(1→4)-β-D-Man*p*A (G−M) and β-D-Man*p*A-(1→4)-α-L-Gul*p*A (M−G) linkages. High field NMR spectroscopy represents a powerful tool for the quantitative determination of reducing end resonances and, thus, for the characterization of the hydrolysis reaction of PolyMG. The degradation of PolyMG at p^{2}H 4.0 and 95 °C monitored by online ^{1}H NMR spectroscopy confirmed that the two linkages in PolyMG considered separately could be described by two first-order rate constants and random degradations. The G−M linkages were hydrolyzed far faster than the M−G linkages in the polymer chain, but the ratio of the rates (k_{G-M}/k_{M-G}) decreased from 12.8 to 6.7 by increasing the pH from 2.8 to 4.5. This is evidence of an intramolecular catalysis of glycosidic cleavage by the undissociated carboxyl groups acting directly as proton donors. The high rate of hydrolysis of the guluronic−mannuronic acid (1→4) linkages in PolyMG is most likely explained by the stabilization of the undissociated carboxyl groups on the mannuronic acid residues, by hydrogen bonds to the 2-OH and 3-OH groups of the preceding guluronic acid residues. The observed greater decrease of k_{G-M} than k_{M-G} in the pH range 2.8−4.5 reflects the difference in pK_a values of the two uronic acids. Because of the more dissociated carboxyl groups of mannuronic acid residues, the cleavage of the G−M glycosidic linkages is affected more than the M−G linkages by increasing the pH to 4.5.

The mechanism of hydrolysis of PolyMG can be utilized to make MG-oligosaccharides mainly with an even number of residues. The G−M linkages being the fastest degraded, the most oligomers will thus have an M on the nonreducing and a G on the reducing end. Following hydrolysis of PolyMG at pH 3.5 and 95 °C, where the ratio of the rates k_{G-M}/k_{M-G} is 10.7, separation of the MG-hydrolysate by SEC and characterization of oligosaccharide fractions by ESI-MS and NMR spectroscopy confirmed this. However, the extra 6% MM content in the polymer was contributing to the weight distribution of chain lengths such that more oligomers with an odd number of residues than expected were obtained. Internal and nonreducing end MM sequences in the odd numbered oligosaccharide fractions were confirmed by NMR spectroscopy. In addition, a lower degradation rate constant for M−M than G−M linkages by a factor of 3.8 at pH 3.5 suggests that the present M blocks (mostly MM dimers) influence the weight distribution of oligomers in the hydrolysate by changing the degradation pattern such that two rapid G−M cleavages also give irregular odd numbered oligomers. The oligosaccharide fractions with an even number of residues consisted of more than 90% strictly alternating oligomers with M on the nonreducing and G on the reducing end. Even numbered oligomers were uniform in chain lengths determined by ESI-MS, whereas in the odd counterparts lower homologues were present mainly attributable to the smaller size and collection of SEC fractions. The chemical shifts (ppm) for the specific residues of MG oligomers (DP2−DP5) were elucidated by 2D ^{1}H and ^{13}C NMR. Well-defined MG oligosaccharides with various chain lengths can be useful in many applications, for example in the study of enzymes such as mannuronic and guluronic acid β-eliminases (lyases) or mannuronan C-5 epimerases.

Acknowledgment. This work was funded by a grant from the Norwegian Research Council. We are very grateful to Bjørn Larsen and Hans Grasdalen (both at NTNU) for valuable discussions, Sissel Tove Ødegaard (NTNU) for technical assistance, and Catherine Taylor (NTNU) for proof reading the manuscript.

References and Notes

(1) Painter, T. J. In *The Polysaccharides*; Aspinall, G. O., Ed.; Academic Press: New York, 1983; Vol. 2, pp 195−285.
(2) Gorin, P. A. J.; Spencer, J. F. T. *Can. J. Chem.* **1966**, *44*, 993−998.
(3) Govan, J. R. W.; Fyfe, J. A. M.; Jarman, T. R. *J. Gen. Microbiol.* **1981**, *125*, 217−220.
(4) Ertesvåg, H.; Doseth, B.; Larsen, B.; Skjåk-Bræk, G.; Valla, S. *J. Bacteriol.* **1994**, *176*, 2846−2853.
(5) Ertesvåg, H.; Høidal, H. K.; Hals, I. K.; Rian, A.; Doseth, B.; Valla, S. *Mol. Microbiol.* **1995**, *16*, 719−731.
(6) Svanem, B. I. G.; Skjåk-Bræk, G.; Ertesvåg, H.; Valla, S. *J. Bacteriol.* **1999**, *181*, 68−77.
(7) Høidal, H. K.; Ertesvåg, H.; Skjåk-Bræk, G.; Stokke, B. T.; Valla, S. *J. Biol. Chem.* **1999**, *274*, 12316−12322.
(8) Hartmann, M.; Holm, O. B.; Johansen, G.-A. B.; Skjåk-Bræk, G.; Stokke, B. T. *Biopolymers* **2002**, *63*, 77−88.
(9) Hartmann, M.; Duun, A. S.; Markussen, S.; Grasdalen, H.; Valla, S.; Skjåk-Bræk, G. *Biochim. Biophys. Acta* **2002**, *1570*, 104−112.
(10) Ertesvåg, H.; Høidal, H. K.; Skjåk-Bræk, G.; Valla, S. *J. Biol. Chem.* **1998**, *273*, 30927−30932.
(11) Holtan, S.; Bruheim, P.; Skjåk-Bræk, G. *Biochem. J.* **2006**, *395*, 319−329.
(12) Thibault, J.-F.; Renard, C. M. G. C.; Axelos, M. A. V.; Roger, P.; Crépeau, M.-J. *Carbohydr. Res.* **1993**, *238*, 271−286.
(13) Haug, A.; Larsen, B.; Smidsrød, O. *Acta Chem. Scand.* **1966**, *20*, 183−190.
(14) Smidsrød, O.; Haug, A.; Larsen, B. *Acta Chem. Scand.* **1966**, *20*, 1026−1034.
(15) Smidsrød, O.; Larsen, B.; Haug, A. *Carbohydr. Res.* **1967**, *5*, 371−372.
(16) Smidsrød, O.; Larsen, B.; Painter, T.; Haug, A. *Acta Chem. Scand.* **1969**, *23*, 1573−1580.
(17) Campa, C.; Holtan, S.; Nilsen, N.; Bjerkan, T. M.; Stokke, B. T.; Skjåk-Bræk, G. *Biochem. J.* **2004**, *381*, 155−164.
(18) Gimmestad, M.; Sletta, H.; Ertesvåg, H.; Bakkevig, K.; Jain, S.; Suh, S.; Skjåk-Bræk, G.; Ellingsen, T. E.; Ohman, D. E.; Valla, S. *J. Bacteriol.* **2003**, *185*, 3515−3523.
(19) Ertesvåg, H.; Skjåk-Bræk, G. In *Methods in Biotechnology*; Bucke, C., Ed.; Humana Press Inc.: Totowa, NJ, 1999; Vol. 10, pp 71−78.
(20) Grasdalen, H. *Carbohydr. Res.* **1983**, *118*, 255−260.
(21) Grasdalen, H.; Larsen, B.; Smidsrød, O. *Carbohydr. Res.* **1977**, *56*, C11−C15.
(22) Grasdalen, H.; Larsen, B.; Smidsrød, O. *Carbohydr. Res.* **1981**, *89*, 179−191.

(23) Ballance, S.; Holtan, S.; Aarstad, O. A.; Sikorski, P.; Skjåk-Bræk, G.; Christensen, B. E. *J. Chromatogr. A* **2005**, *1093*, 59−68.
(24) Glasoe, P. K.; Long, F. A. *J. Phys. Chem.* **1960**, *64*, 188−190.
(25) Holme, H. K.; Lindmo, K.; Kristiansen, A.; Smidsrød, O. *Carbohydr. Pol.* **2003**, *54*, 431−438.
(26) Haug, A. *Report No. 30;* Norwegian Institute of Seaweed Research: Trondheim, 1964.
(27) Grasdalen, H.; Larsen, B.; Smidsrød, O. *Carbohydr. Res.* **1979**, *68*, 23−31.
(28) Wiberg, K. B. *Chem. Rev.* **1955**, *55*, 713−743.
(29) Szejtli, J. *Säurehydrolyse glykosidischer Bindungen;* Akadémiai Kiadó: Budapest, 1976.
(30) Sharon, N. *Complex Carbohydrates*; Addison-Wesley Publishing Company Inc.: Reading, MA, 1975; pp 56−65.
(31) Heyraud, A.; Gey, C.; Leonard, C.; Rochas, C.; Girond, S.; Kloareg, B. *Carbohydr. Res.* **1996**, *289*, 11−23.
(32) Larsen, B.; Smidsrød, O.; Haug, A.; Painter, T. *Acta Chem. Scand.* **1969**, *23*, 2375−2388.

BM050984Q